

ChemCam investigation of the John Klein and Cumberland drill holes and tailings, Gale crater, Mars



R.S. Jackson^{a,*}, R.C. Wiens^b, D.T. Vaniman^c, L. Beegle^d, O. Gasnault^{e,f}, H.E. Newsom^a, S. Maurice^{e,f}, P.-Y. Meslin^{e,f}, S. Clegg^b, A. Cousin^f, S. Schröder^f, J.M. Williams^g

^a Department of Earth and Planetary Science, University of New Mexico, Albuquerque, NM 87131, USA

^b Los Alamos National Laboratory, Los Alamos, NM 87545, USA

^c Planetary Science Institute, 1700 East Fort Lowell, Suite 106, Tucson, AZ 85719, USA

^d Jet Propulsion Laboratory, California Institute of Technology, Pasadena, CA 91109, USA

^e IRAP, UPS-OMP, Université de Toulouse, 31000 Toulouse, France

^f IRAP, CNRS, 9 avenue du Colonel Roche, BP 44346, F-31028 Toulouse CEDEX 4, France

^g Western Washington University, 516 High St, Bellingham, WA 98225, United States

ARTICLE INFO

Article history:

Received 27 August 2015

Revised 19 April 2016

Accepted 19 April 2016

Available online 13 May 2016

Keywords:

Experimental techniques

Mars

Mars, surface

ABSTRACT

The ChemCam instrument on the Mars Science Laboratory rover analyzed the rock surface, drill hole walls, tailings, and unprocessed and sieved dump piles to investigate chemical variations with depth in the first two martian drill holes and possible fractionation or segregation effects of the drilling and sample processing. The drill sites are both in Sheepbed Mudstone, the lowest exposed member of the Yellowknife Bay formation. Yellowknife Bay is composed of detrital basaltic materials in addition to clay minerals and an amorphous component. The drill tailings are a mixture of basaltic sediments and diagenetic material like calcium sulfate veins, while the shots on the drill site surface and walls of the drill holes are closer to those pure end members. The sediment dumped from the sample acquisition, processing, and handling subsystem is of similar composition to the tailings; however, due to the specifics of the drilling process the tailings and dump piles come from different depths within the hole. This allows the ChemCam instrument to analyze samples representing the bulk composition from different depths. On the pre-drill surfaces, the Cumberland site has a greater amount of CaO and evidence for calcium sulfate veins, than the John Klein site. However, John Klein has a greater amount of calcium sulfate veins below the surface, as seen in mapping, drill hole wall analysis, and observations in the drill tailings and dump pile. In addition, the Cumberland site does not have any evidence of variations in bulk composition with depth down the drill hole, while the John Klein site has evidence for a greater amount of CaO (calcium sulfates) in the top portion of the hole compared to the middle section of the hole, where the drill sample was collected.

© 2016 Elsevier Inc. All rights reserved.

1. Introduction

The ChemCam instrument on the Mars Science Laboratory (MSL) rover, also called *Curiosity*, consists of a Laser Induced Breakdown Spectroscopy (LIBS) instrument which allows for $\sim 400 \mu\text{m}$ diameter chemical analyses from 1.5 m to 7.0 m away, as well as a panchromatic Remote Micro Imager (RMI) for context. These analyses provide geochemical context for the mineralogical analysis of drill samples by the internal instruments, Chemistry and Mineralogy (CheMin) and Sample Analysis at Mars (SAM); furthermore,

the fine spatial resolution of ChemCam, as applied to veins and other fine-scale diagenetic features, provides an important complement to the bulk composition from the internal instruments or the Alpha Particle X-Ray Spectrometer (APXS), e.g., McLennan et al. (2014); Mangold et al. (2015).

After landing on Mars, the Curiosity rover briefly drove away from its main science objective of Mount Sharp and towards a secondary science objective at Yellowknife Bay. The objective in this detour was to sample a local region of higher thermal inertia observed from orbit, which turned out to be exposed sandstone and mudstone, in contrast to the gravelly surface of the Bradbury Rise on which the rover landed (Grotzinger et al., 2014).

Yellowknife Bay was topographically the lowest point on the rover traverse. This campaign included drilling into two locations

* Corresponding author. Tel.: +1 5052698411.

E-mail address: ryansteelejackson@yahoo.com, rjacks04@unm.edu (R.S. Jackson).

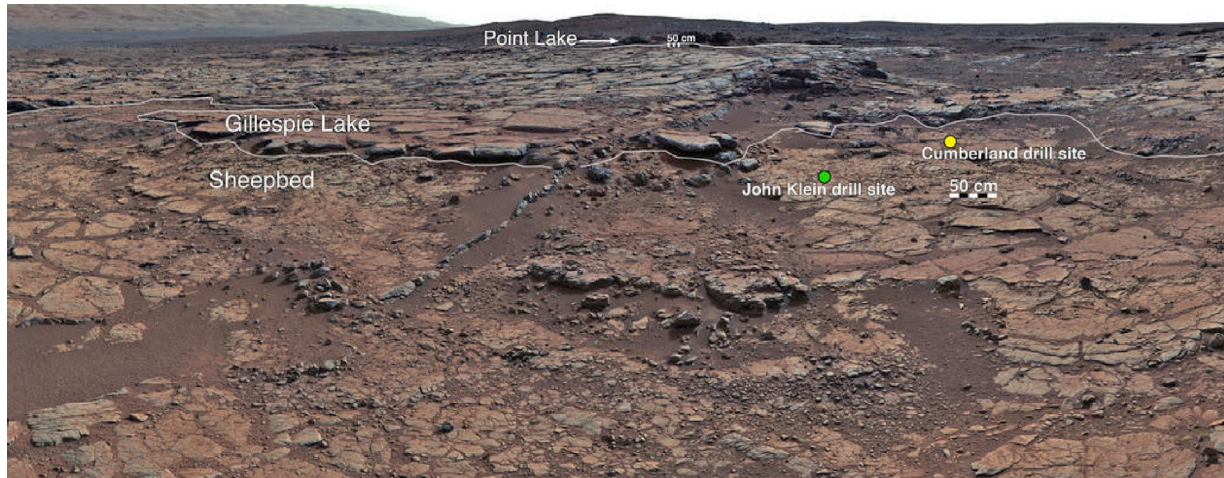


Fig. 1. MastCam mosaic of the Yellowknife Bay formation with the two drill sites marked with the colored circles.

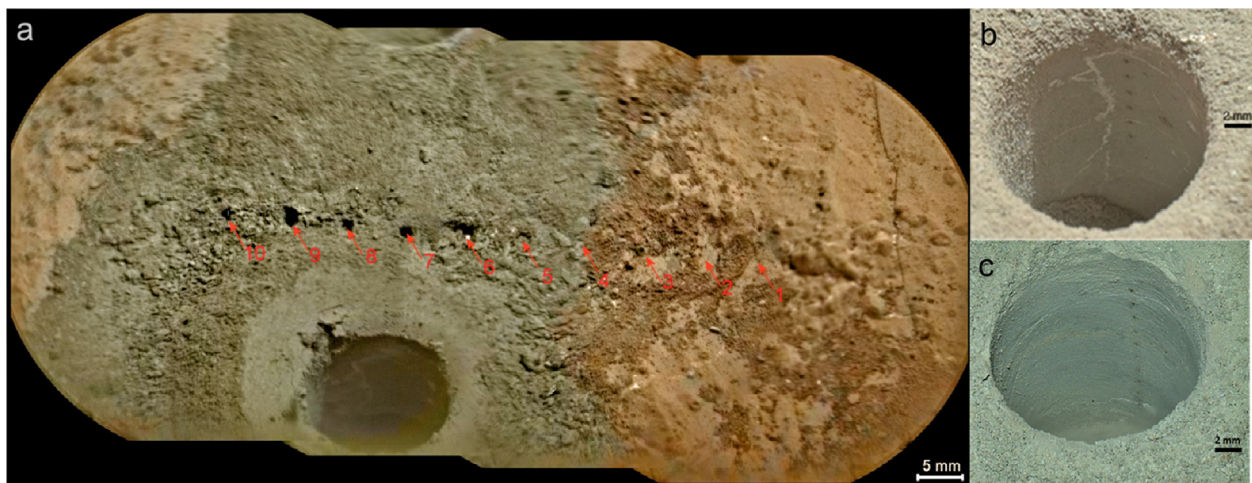


Fig. 2. (a) Merged RMI and MastCam mosaic of the John Klein drill hole and tailings. The tailings are grey on top of the red surficial dust. (b) MaHLI image of the John Klein Drill hole, veins and pits from the ChemCam laser. (c) MaHLI image of the Cumberland Drill hole, veins and divots from the ChemCam laser. (For interpretation of the references to colour in this figure legend, the reader is referred to the web version of this article.).

in the Sheepbed Mudstone, termed John Klein and Cumberland; ChemCam was used to characterize the surface of the drill target, the walls of drill holes, and drill tailings. Fig. 1 displays a MastCam mosaic of Yellowknife Bay with the drill sites marked, and Fig. 2 is a RMI mosaic (Le Mouelic et al., 2015) of the John Klein drill hole and tailings, as well as MaHLI images of the drill hole walls. The results of this first use of the drill sampling system, including the nearby Cumberland drill hole, confirmed that the Sheepbed unit represented an ancient lacustrine environment (e.g., Grotzinger et al., 2014). The Sheepbed unit in the areas around the rover traverse, including the vicinity of the drill holes contains veins, nodules, and Mg-rich ridges (Stack et al., 2014; Léveillé et al., 2014; Nachon et al., 2014). The veins are fracture-fill material within the Sheepbed Mudstone; they have calcium sulfate composition and consist of the minerals anhydrite and bassanite (Nachon et al., 2014; Vaniman et al., 2014). The nodules are roughly spherical diagenetic features likely to be concretions with Fe-rich cement (likely magnetite), formed from aqueous alteration of the mudstone by diagenetic pore fluids, and having a composition not greatly dissimilar to the mudstone (Stack et al., 2014). The Mg-rich ridges are diagenetic features in the mudstone that are more resistant

to erosion than the rock; the ridges have a composition similar to smectite clays with cement layers and are enriched in Mg (Léveillé et al., 2014; Siebach et al., 2014).

Because the sample provided to the rover's internal instruments at each site is a small amount of material from a specific portion of the drill hole (the lower portion), an important question is whether this sample has the same composition as the materials analyzed by ChemCam and APXS at the surface near the drill sites, and by ChemCam down the upper portion of the drill holes, especially given the presence of the diagenetic features. The elemental composition of rock sampled near the hole is used to infer the composition of the x-ray amorphous phase (e.g., Morris et al., 2015), assuming that the nearby chemistry is the same as that of the lower portion of the drill hole. If they in fact differ, the inferred amorphous composition will be incorrect. ChemCam has the unique capability of understanding compositional differences within the drill hole as well as the tailings and dump pile. This paper presents a detailed examination of the ChemCam analyses of the drill target, thereby providing an important chemical context for the analysis of the drill samples by the CheMin and SAM experiments (Vaniman et al., 2014; Ming et al., 2014).

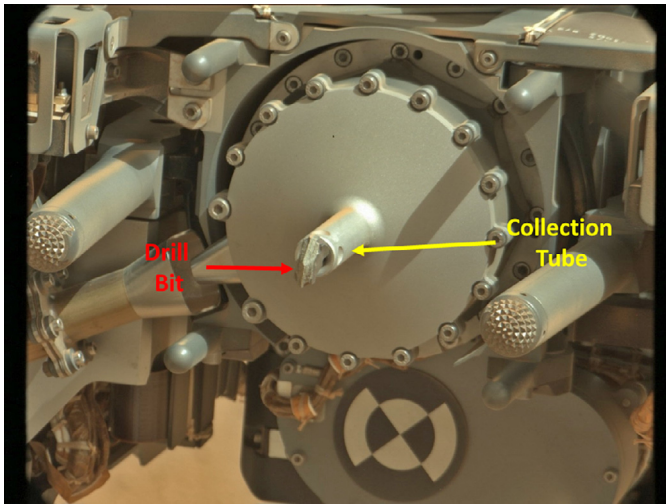


Fig. 3. MastCam image of the drill bit after the Cumberland sample was drilled. The diameter of the drill bit is 1.6 cm and the collection tube is 1.4 cm. Once the drill progresses ~1.5 cm into the sample, the collection tube engages the bore hole and sample collection begins. From that point until full drill depth, the majority of created fines created in the drilling process are forced between the flutes and collection tube where they are eventually collected inside the drill bit assembly. Martian fines that are created at depths > 2.0 cm tend not to make it to the surface due to the firm packing of fines from shallower depth between the collection tube and borehole.

2. Analytical methods

2.1. Drilling process

The MSL Sample Acquisition, Processing, and Handling (SA/SPaH) Subsystem utilizes a rotary-percussive drill to create fines and collect samples in 1 single step (Okon, 2010). The Powder Acquisition Drill System (PADS) was designed to collect fines from depths below 2.0 cm to a maximum depth of 6.5 cm. The drill stem is made up of two parts, (1) a commercial hammer drill bit at the end of the drill stem that consists of deep flutes specifically designed for aggressive cutting removal and (2) a sample collection tube which is fitted on the outside of the drill stem. This collection tube is designed such that created fines are forced up the flutes and into the sample collection reservoir (Anderson et al., 2012). The cutting tip and percussion loads are designed to generate fine particles < 150 micron for the CheMin and SAM instruments. During testing of this drill it has been shown that 30–90% of all particles produced are less than the 150 micron particle diameter, and virtually all are less than 0.1 cm (Anderson et al., 2012).

The Powder Acquisition Drill System PADS is designed to leave fines that are created at the start of drilling on the rock surface (Anderson et al., 2012). As the rotary-percussive drill action begins, the cutting tip creates fines that move onto the rock surface where they migrate following natural slopes in the target rock. Once the drilling process reaches a depth of ~1.5 cm, the collection tube first engages the borehole and a seal begins to form between the collection tube and borehole (Fig. 3). At ~2.0 cm of depth, the seal between the borehole and collection tube becomes tight and the collection efficiency greatly increases as fines are forced into the region between the flutes and collection tube as the drill penetrates into the rock. Validation of the design of the PADS was performed utilizing flight hardware in a martian environmental chamber. These tests show that very little material emanates from the borehole after 2.0 cm of drill penetration and that > 90% of all fines that make it into the collection chamber are from depths below 2.0 cm.

Table 1

Table of abbreviations used in the paper.

Table of abbreviations	
Abbr.	Meaning
MSL	Mars Science Laboratory
LIBS	Laser Induced Breakdown Spectroscopy
RMI	ChemCam Remote Micro Imager
CheMin	Chemistry and Mineralogy (X-Ray Diffraction instrument on MSL)
SAM	Sample Analysis at Mars (Suite of Chemistry instrument on MSL)
APXS	Alpha Particle X-Ray Spectrometer (Contact chemistry instrument on the rover arm)
MaHLI	Mars Hand Lens Instrument
PADS	Powder Acquisition Drill System
SA/SPaH	MSL's Sample Acquisition, Processing, and Handling Subsystem
DRT	Dust Removal Tool, a wire brush

At both John Klein and Cumberland sites, the depth the drill reached was 6.5 cm. At the end of the drilling process, visual imaging shows that there are fines left within the borehole made of material that either did not make it into the collection tube or were part of the seal between the collection tube and borehole and fell back into the hole. On Mars at Cumberland and John Klein, and in environmental laboratory testing, the act of retracting the drill bit left a borehole that is dust and fine free with residual fines in the bottom of the borehole. In a typical 6.5 cm hole, approximately 3.5 cm of fines are observed still in the borehole by MaHLI. Recent drill holes in the Murray formation in Marias Pass have exhibited a coating on the drill hole wall, which can be dislodged by ChemCam LIBS shots.

In summary, material from the first ~15 mm of drilling constitute the primary tailings material visible to APXS on the surface surrounding the hole after drilling, with some contribution of material generated from depths of between 1.5 cm and 2.0 cm. Fines created from below 2.0 cm are predominantly collected and fed into the two analytical instruments SAM and CheMin Table 1.

2.2. Timeline of operations

The ChemCam sequences and the drilling operations are listed in Table 2 and described in the next section. The drilling operations began on sol 180 when a shallow hole, or “mini-hole”, 2 cm deep, was drilled into the John Klein site in order to ensure that drilling into the rock would pose no danger to the mechanisms. After the test hole was successful the rover drilled a full size hole, 6.5 cm deep and 1.6 cm in diameter, in John Klein. After the John Klein bulk sample obtained by the drill was analyzed by the internal instruments CheMin and SAM, an un-sieved pile and a pile of tailings sieved with a 150 μm size sieve were dumped back to the ground; the hole and tailings were observed by the geochemistry instruments (ChemCam and APXS) and the suite of cameras onboard. The rover then moved ~3 m to the Cumberland site, where another hole was drilled (on sol 279) and a similar series of observations was conducted, including bulk analysis of the drill sample by the internal instruments and characterization of the drill tailings and hole by external instruments. In the two drill samples, the CheMin X-Ray Diffraction investigation detected plagioclase (plus minor sanidine), Fe-forsterite, augite, pigeonite, orthopyroxene, magnetite, pyrrhotite, akaganeite, and calcium sulfates (anhydrite and bassanite); the smectite clay and amorphous

Table 2

Table of ChemCam analyses at the drill sites, as well as, the drilling campaign at each site. The Cumberland material was stored within the over for over 200 sols for further investigation by the internal instruments before being dumped, while John Klein material was dumped before the drive to the Cumberland site.

Table of Sheepbed mudstone drill operations						
Sequence ID	ChemCam points	Shots per point	Site	Target	Sol	Distance
CCAM01155	5	30	John Klein	Rock	155	5.41 m
CCAM02165	9	50	John Klein	Rock	165	3.51 m
CCAM03165	9	50	John Klein	Rock	165	2.99 m
Drive to John Klein					166	
John Klein Drilling					181	
CCAM02183	10	30	John Klein	Tailings	183	2.48 m
CCAM02195	5	50	John Klein	Tailings	195	2.48 m
CCAM01227	10	30	John Klein	Drill Hole Wall	227	2.47 m
CCAM02227	5	30	John Klein	Tailings	227	2.49 m
CCAM01234	10	30	John Klein	Tailings/Dump Pile	234	2.49 m
CCAM01187	16	30	Cumberland	Rock	187	2.60 m
CCAM01274	5	30	Cumberland	Rock	274	2.90 m
CCAM01275	9	30	Cumberland	Rock	275	2.37 m
CCAM02275	9	30	Cumberland	Rock	275	2.35 m
CCAM01277	16	30	Cumberland	Rock	277	2.40 m
Drive to Cumberland site					274	
Cumberland Drilling					279	
CCAM01281	10	30	Cumberland	Tailings	281	2.40 m
CCAM07284	10	30	Cumberland	Drill Hole Wall	285	2.41 m
CCAM02289	5	50	Cumberland	Tailings	289	2.38 m
CCAM01292	5	100	Cumberland	Rock	293	2.28 m
CCAM04292	9	50	Cumberland	Rock	294	2.35 m
Cumberland Sample Dumped					486	
CCAM01488	10	30	Cumberland	Dump Pile	488	2.37 m
CCAM02488	5	30	Cumberland	Dump Pile	488	2.39 m

component account for roughly 50 weight percent of both drill samples (Vaniman et al., 2014).

The ChemCam portion of the drilling campaign included 3 sequences on the John Klein rock surface, 4 sequences in the John Klein tailings including 1 sequence into the dump pile, and 1 sequence on the drill hole wall; in addition, ChemCam ran 7 sequences on the Cumberland rock, 2 sequences in the Cumberland tailings, 1 sequence on the drill hole wall, and two sequences in the Cumberland dump pile. Due to the view angle, the direct ChemCam observations only covered approximately the upper 1–1.3 cm of the drill hole walls, thus not providing information down the whole depth of the hole that remains exposed. Sieved and un-sieved sediment in the SA/SPaH was dumped after portions were delivered for analysis by SAM and CheMin; dump piles were then analyzed by ChemCam. The John Klein sample was dumped back onto the John Klein tailings before moving on to the Cumberland location while the Cumberland material was carried by the rover for ~200 sols before being dumped. For both dump piles the first 10 ChemCam laser shots at each observation point were used in this analysis in order to avoid including any rock underneath the piles. As these sequences were run shortly after dumping, there should be little if any inclusion of air fall dust. For the rest of ChemCam data in this study, both averaged and single-shot data are used. Single-shot data is the quantified analysis from each laser shot; this data can have higher uncertainties than the averaged data. Averaged data utilizes a spectrum created by averaging the spectra of all LIBS shots after the first 5, and then this mean spectrum is used to calculate the oxide abundances. By averaging the multiple (usually 25) spectra together it is possible to improve the signal to noise ratio and provide less uncertainty than the single shot data, as this process smooths out the noise in the processed spectrum. The first 5 LIBS shots are automatically ignored by the data processing method in order to eliminate any contribution by air fall dust into the mean spectrum.

2.3. LIBS

ChemCam analyses are planned and organized by individual sequences (which have a unique target name) usually consisting of a line-scan or grid raster pattern of observation points, where each point is observed with multiple laser shots, 30 or 50 in this study, and where an emission spectrum was recorded for each laser shot. For each sequence in this study, 5–10 different points were analyzed (Wiens et al., 2012). The elemental detections from the LIBS spectra are reported in terms of the usual oxide abundances of SiO₂, TiO, Al₂O₃, FeOT (Total Fe as FeO), MgO, CaO, Na₂O, and K₂O. The abundances were quantified from the spectra by using a calibration method (Clegg et al., 2016, in preparation) which uses both the PLS1 algorithm (Clegg et al., 2009; Wiens et al., 2013) and independent component analysis (Forni et al., 2013). In this study S is not quantified directly. However, its presence in significant quantities can be inferred when major-element totals well below 100% are reported. The “missing component” in these cases is the reported major-element total subtracted from 100%; this is used as a proxy for S in graphs and is supported by the detection of sulfides and calcium sulfates by CheMin (Vaniman et al., 2014), but the missing component also includes H₂O, Cl, and all other minor elements that are not quantified by the current version of the ChemCam calibration method. In contrast APXS normalizes all their data to 100% making the assumption that all major components are accounted for in the analysis (Gellert and Clark, 2015; Gellert et al., 2006).

The LIBS technique vaporizes a small amount of material with each laser shot, so that successive shots penetrate deeper into the material. By analyzing successive spectra one can determine how the composition of the material changes with depth on a scale of microns in rocks and millimeters in loose material. In loose sediment such as the tailings and dump pile, the LIBS shots can “dig” through the material into the rock underneath even in sequences of only 30 shots per point (Lanza et al., 2015). The transition



Fig. 4. (a) Location of the Wernecke target, showing its location in reference in the John Klein Drill Hole (b) MaHLI image of the Wernecke target after the dust was removed by the dust removal tool on the rover's arm. This shows that the red coloration at John Klein and Cumberland is due to the dust, and the mudstone itself is grey; in addition, veins and nodules are visible at the surface. (For interpretation of the references to colour in this figure legend, the reader is referred to the web version of this article.).

between loose material and rock can be determined by observing the hydrogen emission lines in the ChemCam spectra to identify the tailings which show evidence of hydration and excluding all shots after there is a drop in hydration of material (Schröder et al., 2015).

3. Results

3.1. Surface material

Unless disturbed by brushing or by LIBS shots the red color of the surfaces seen in most of the images is not the color of the rocks themselves, but is the result of nearly complete coating by air fall dust. This can be seen at the target Wernecke (Fig. 4), which is near the John Klein drill hole in the Sheepbed Mudstone. Wernecke was brushed clean by the rover DRT (Dust Removal Tool) on the Rover arm prior to characterization by APXS and ChemCam; the red dust was cleared away exposing the underlying grey rock, thus the red coating is only dust and not an alteration layer at the surface of the rock.

In total, 480 individual location points were analyzed in the Sheepbed Mudstone by ChemCam (Mangold et al., 2015). The surface rock of the drill sites was characterized through imaging and by some of these ChemCam analyses; MaHLI imagery revealed several veins and nodules at the surface at both sites (Fig. 5). However, this paper will only focus on diagenetic features observed in the ChemCam data at the surface in the immediate vicinity of the drill sites; the two dominant diagenetic features are calcium sulfates and Mg-rich ridges. While nodules (defined from Stack et al., 2014) are visible in the MastCam image in Fig. 5b, they are not distinct in the ChemCam compositional data. This is supported by the work from Stack et al. (2014), who also concludes that the nodule rich Sheepbed Mudstone is not chemically different than the nodule-free mudstone. Fig. 6 illustrates the relative amounts of diagenetic influence at the surface of the two drill sites. As seen in Fig. 6a the distribution of CaO at Cumberland tends to show higher values than the John Klein data, indicating a greater amount of CaO veins. On the other hand, Fig. 6b provides evidence for a greater distribution of the Mg-rich ridges at the John Klein surface rather than the Cumberland site.

Where the Mg-ridges are observed the MgO/Al₂O₃ ratio values are greater than 1.5 (Léveillé et al., 2014). The values of the tailings in context with the surface observations are shown in Fig. 7; Fig. 7c displays a grouping of samples with high MgO values at the surface which are consistent with what was seen in Fig. 6b.

3.2. Drill hole and tailings

The walls of the two drill holes are clearly different in appearance, as seen in Fig. 8a and b. In the John Klein drill hole, many white veins and nodules are visually distinct from the grey bulk rock, but at Cumberland the veins and nodules are less abundant. This visual assessment is quantitatively supported by the sulfates detected by CheMin, 3.6% at John Klein and 1.5% at Cumberland, and by mapping of the drill hole walls, from which a vein surface area fraction of 5.18% is calculated at John Klein and 1.74% at Cumberland (Vaniman et al., 2014). There were sequences of ChemCam observations down both drill hole walls, but as stated earlier, the two sequences only sampled approximately the top centimeter, and do not provide a complete understanding of the entire holes. Fig. 8c shows the detection of at least 2 veins on the John Klein wall but no observations of the calcium sulfates within Cumberland; Fig. 8d does provide limited evidence for materials similar to the Mg-rich ridges in both drill hole walls.

Previously published work has shown that the Sheepbed Mudstone is comprised of mostly unaltered basaltic materials and roughly 20% smectite clay (Grotzinger et al., 2014; Vaniman et al., 2014). This is also shown by the correlation between SiO₂, FeO_T that can be observed in Fig. 9a. This trend could be explained by a mixture between a low-Si and low-Fe component, the Ca sulfate, and a moderate-Si and relatively high-Fe component such as a mafic primary silicate or a Fe-rich smectite. Fig. 9b shows an anti-correlation between combined SiO₂ and FeO_T, and CaO, representing a mixing trend between alteration material–calcium sulfate veins—and the bulk component. This mixing trend is shown in greater detail in Fig. 7a which shows two distinct groups of material sampled when the rock and drill hole wall were shot. However, there is scatter in the value of the missing component as it contains signal from not just sulfur but also other elements besides the 8 oxides reported in the major-element totals. In addition, a distinct gap is shown in Fig. 7a; this gap is representative of the difference between the host rock and calcium sulfate veins and is bridged by the drill tailings as seen in Fig. 7b which shows the same parameters for the drill tailings. The values in the drill tailings stretch from roughly the top right of the main cluster of values in the lower left of Fig. 7a, representing the basaltic-like mudstone, towards the lowest values identified as containing sulfate material (Fig. 7a); thus the drill tailings show a mixing trend between the mudstone and alteration materials. The low silica trend is present in Fig. 7c as well (encircled with the solid line); however, it also includes a trend with similar silica values to the mudstone sediments but with much greater MgO content (encircled with the dotted line). This is in agreement with the MgO trend that was observed in Fig. 6b. There are a few points in the drill tailings that suggest some mixing of the Mg-rich ridges into the drill tailings, but this trend is not as prominent as the trend indicating the inclusion of calcium sulfate veins into the drill tailings (Fig. 7d).

For both dump piles only the first 10 shots at each observation point were used in the analysis in order to avoid including any surface material underneath the piles. The interesting observation by Schröder et al. (2015) that powdered material (both fine-grained soil and drill tailings) appears to have more highly variable H emission intensity than solid material provides a useful indication of whether LIBS shots are sampling the drill tailings

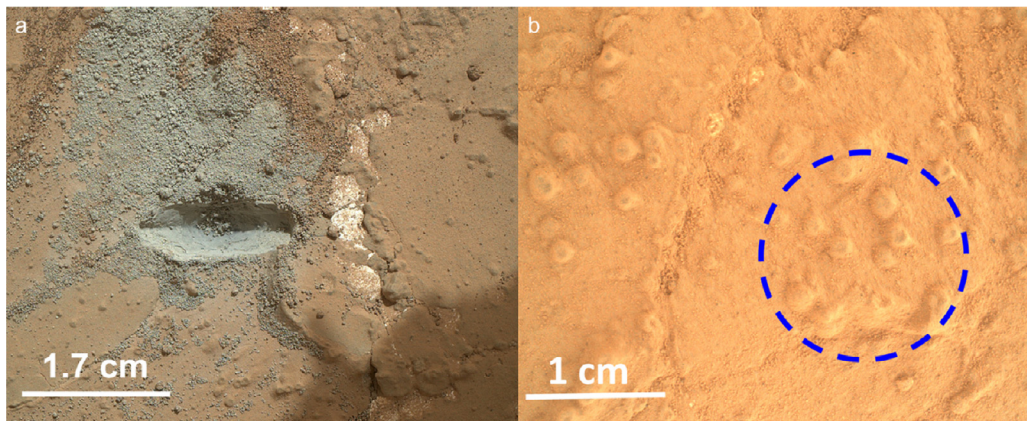


Fig. 5. (a) MaHLI of John Klein after the first drill bit test, white vein material is easily identified (b) MaHLI of Cumberland before drilling; several nodules can be located in this site. The dotted circle is the location of the APXS observation.

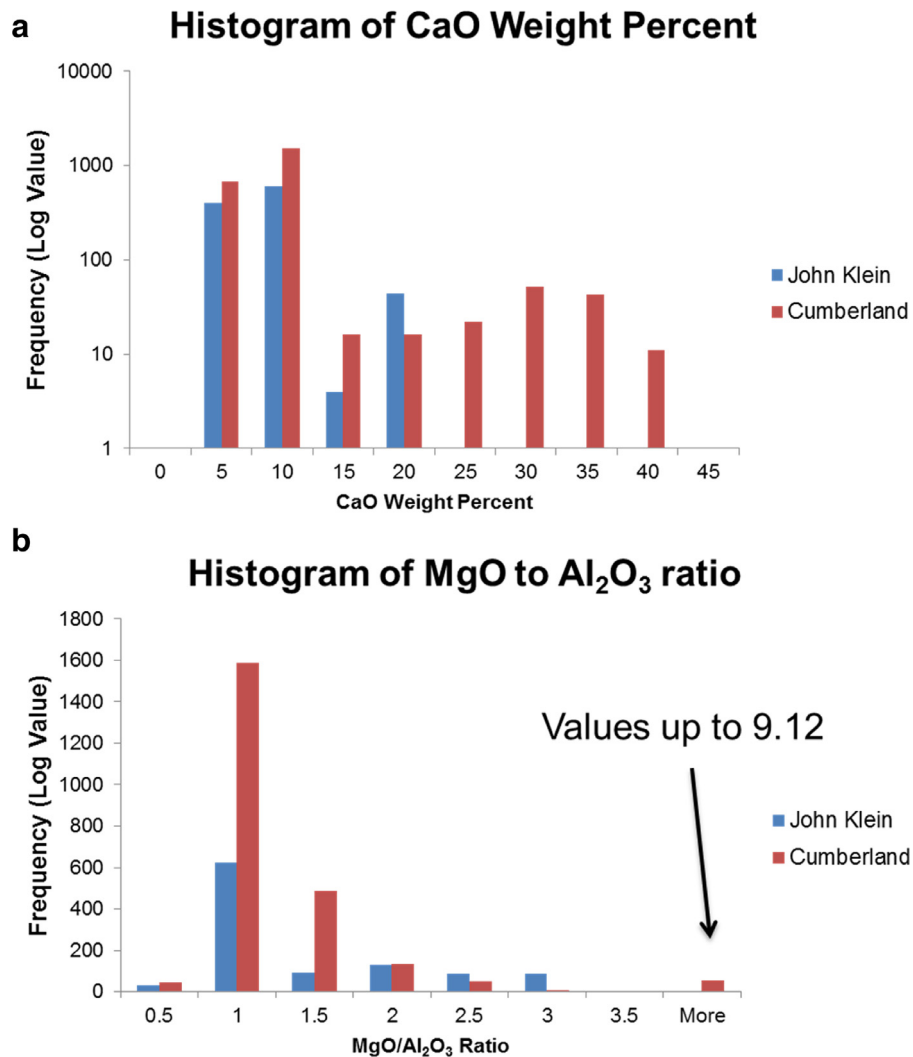


Fig. 6. Histograms of single shot data on the surfaces of the drill sites (a) displays the distribution of CaO weight percent at the two sites, values above 15% provide evidence of calcium sulfate veins (b) displays the MgO to Al_2O_3 ratio at the two drill sites, values of 1.5 or above provide evidence of Mg-rich ridges.

or the solid rock below them. Schröder et al. (2015) data demonstrates a strong drop off in hydration after the 10th shot for all of the observation points in the John Klein dump pile suggesting that the fines were penetrated. Fig. 10 illustrates the difference between the drill tailings and dump pile, in John Klein there is a tendency for the dump pile to be higher in the missing component

and CaO and lower in SiO_2 and FeO_T indicating higher amount of calcium sulfates (Fig. 10a and c). In Cumberland, there are more sequences in the dump pile but there does not seem to be any trend differentiating the dump pile from the drill tailings although the FeO_T composition is more variable in the dump pile than in the tailings with several points slightly lower than the

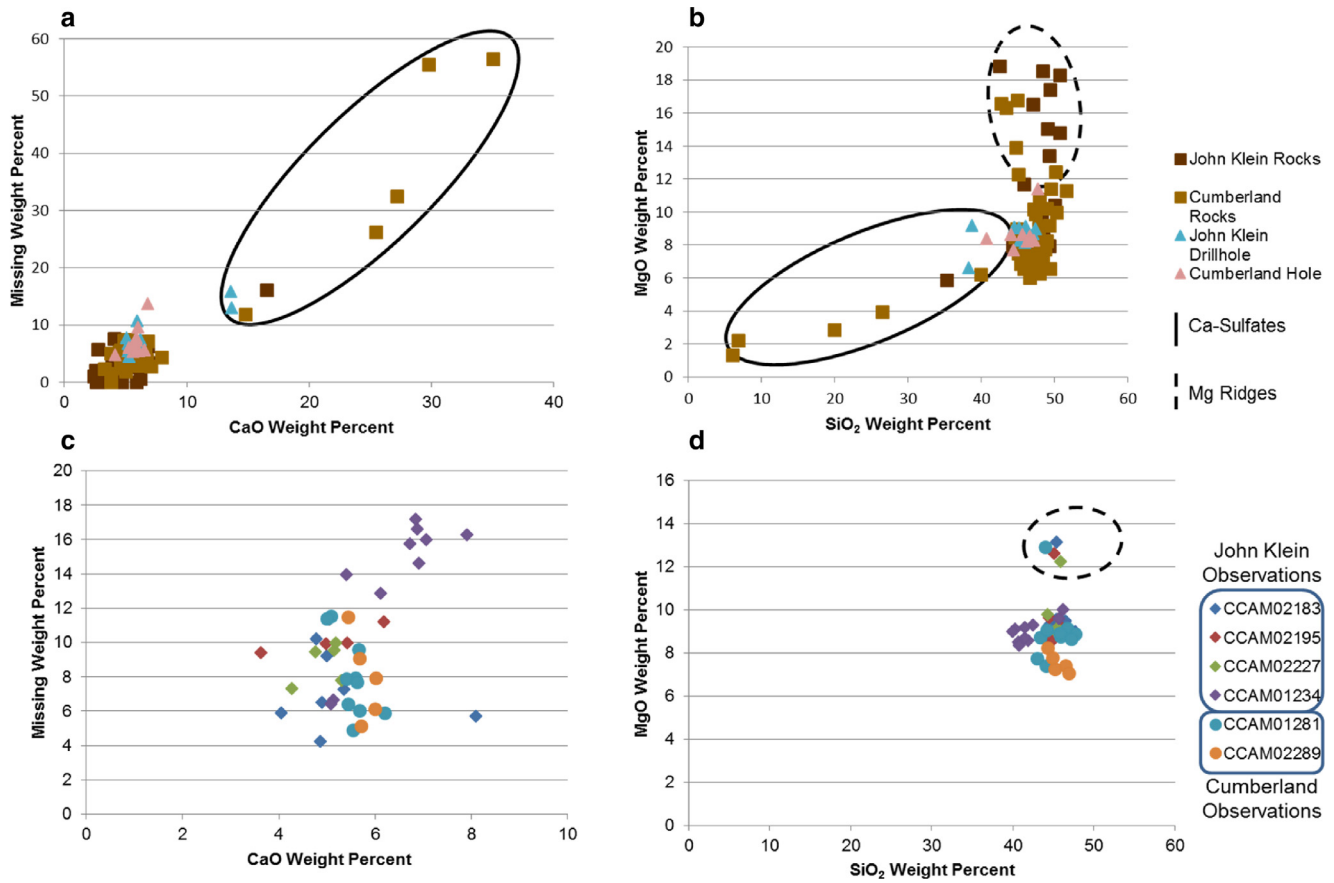


Fig. 7. Averaged data for all observations at John Klein and Cumberland including surface (rocks), drill hole wall, drill tailings, and dump pile. (a) Variation of the missing component (used as a proxy for sulfur) compared to variation in the CaO weight percent in the ChemCam observations of the rock and the drill hole wall. The circled points are best explained as calcium sulfate veins. (b) Variation of the missing component and calcium oxide in the drill tailings; the spread of points indicates a mixing trend between the source rock, represented by the lower left hand cluster in graph “a”, and the high CaO points that were circled in graph “a”. (c) Variation in SiO₂ compared to MgO weight percent in the observations on the rocks and the drill hole wall. The points circled by a solid line are the same as the veins from missing component and calcium oxide graph while the points enclosed by the dashed circle may be explained as Mg-rich ridges. (d) Variation in SiO₂ compared to MgO weight percent for the observations in the drill tailings. The points encircled by the dashed line again are likely representative of Mg-rich ridges.

tailings cluster and four points higher in FeO_T while lower in SiO₂ (Fig. 10b and d).

Fig. 11 displays the average value for each oxide reported by the ChemCam data processing for the drill tailings and dump pile at John Klein and Cumberland with error values indicating 1 standard deviation. The tailings values were calculated by averaging all single shot data from shots within the drill tailings; the dump pile values were calculated by averaging the first 10 LIBS shots in the dump pile; there are not any statistically significant differences between any of the reported oxides besides the CaO percentage of the John Klein dump pile.

3.3. Comparison of results from ChemCam and results of other instruments

Fig. 12 provides a comparison between the APXS and ChemCam results for CaO and SiO₂, to see if the two geochemical instruments are consistent with each other. In addition, this process provides an opportunity to compare bulk chemistry from the drill sites (APXS), to the point data collected by ChemCam. The ChemCam and APXS values of these oxides provide complementary measurements for the two material assemblages analyzed in this research. The greater spread of ChemCam points is to be expected as the LIBS technique samples a very small volume of material with each laser shot (about 400 microns per observation at a distance of 3 m) and the multiple sample points are able to observe much of

the chemical heterogeneity within the rock (Maurice et al., 2012). In contrast, the APXS technique reports a bulk measurement from the instrument's active area that has a diameter of 1.7 cm and a footprint of 2.3 cm² (Gellert and Clark, 2015). The APXS data used here are from the observations conducted at both drill sites, consisting of 9 measurements (McLennan et al., 2014).

One advantage of the ChemCam instrument is its ability to detect the hydrogen signal from water (including water bound in minerals), thus allowing ChemCam to determine from a distance a qualitative estimate of the water content of a sample. The tailings appear enriched in hydrogen but the mudstone itself displayed very low hydration values (Schröder et al., 2015). Recent laboratory studies in a martian atmosphere (A. Cousin, personal communication, June 12, 2015) have shown that material observed as a powder yields a higher H peak than the same material observed as a pressed pellet. Based on these studies it appears that the differences between tailings and drill hole walls are not due to physical processes on Mars. The enriched hydration values in the tailings are similar to values seen in soils, and show no trend with time in different observations taken over several weeks. The observations down both drill hole walls showed low hydration values but Cumberland has a slightly higher value than John Klein (Schröder et al., 2015). These values are consistent with the H₂O abundances reported by the SAM instrument of 1.8–2.4 wt. % in the John Klein material and 1.7–2.5 wt. % in the Cumberland material (Ming et al., 2014).

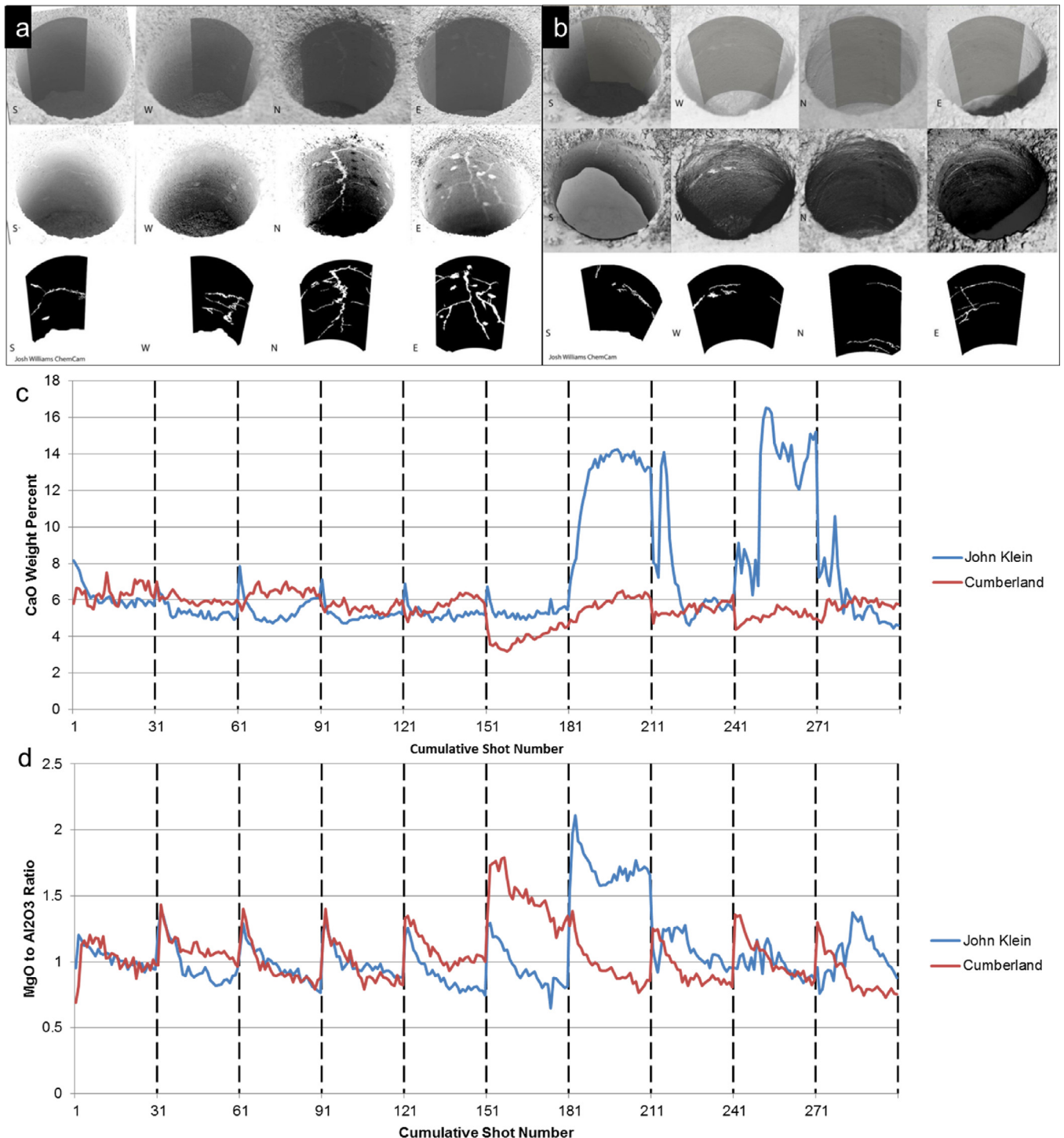


Fig. 8. (a) Mapping of the John Klein drill hole walls showing the prevalence and distribution of veins and nodules. (b) Mapping of the Cumberland drill hole walls showing the distribution of veins and nodules which are much rarer than the same features in John Klein (Vaniman et al., 2014). (c) The variation of calcium oxide abundance in weight percent by shot number, for the sequences down the drill hole wall, CCAM01227 for John Klein (blue line) and CCAM07284 for Cumberland (red line). At point 7 and 9, the enrichment of CaO in the John Klein sequence indicates the possible detection of calcium sulfate veins; however, at no point does the Cumberland sequence give evidence that it encountered any veins. (For interpretation of the references to colour in this figure legend, the reader is referred to the web version of this article.).

4. Discussion

4.1. Drilling process

As stated previously, the drill tailings are almost exclusively from the top 2 cm of the drill hole, while the material sampled by the drill system, including the dump piles and sample portions

for CheMin and SAM, are predominantly from > 2 cm below the surface. This difference in location of the materials allows for a comparison of the geochemistry down the drill hole as seen in Fig. 10. The dump pile material provides evidence for an increase in the amount of calcium sulfates further down the drill hole in John Klein, but does not show a change within Cumberland drill hole except possibly from the surface into the drill hole. These

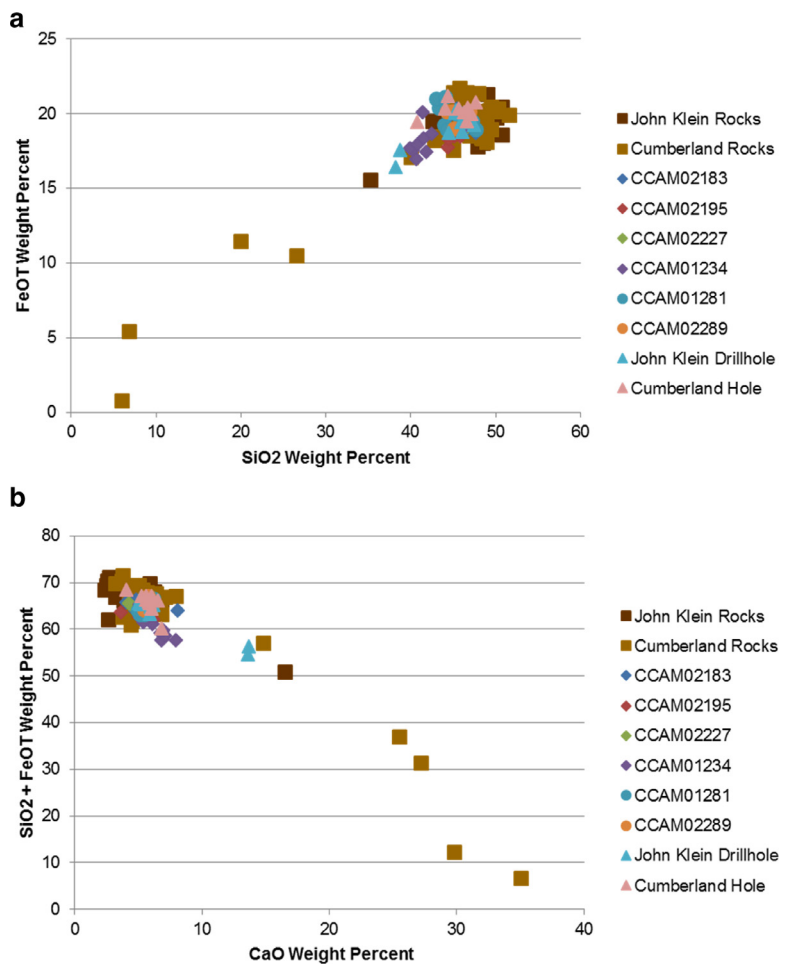


Fig. 9. Averaged data for observations at John Klein and Cumberland including surface (rocks), drill hole wall, and drill tailings, CCAM sequence numbers are shown for drill tailings. (a) Correlation between SiO₂ and FeOT, which is consistent with the bulk rock composed of mostly chemically unaltered basaltic sediment. (b) The anti-correlation between CaO and combined SiO₂ and FeOT. This displays the mixing trend between the mafic silicates that make up the bulk rock of the mudstone and the diagenetic features (Calcium sulfate veins).

quantitative differences are consistent with visual mapping in Fig. 7, but as shown in Fig. 11 are not statistically significant in all cases except for the CaO value of the John Klein Dump Pile.

4.2. John Klein and Cumberland

Figs. 8 and 9 display a mixing trend within the drill tailings; this is most evident in Fig. 9b where the silicate component is represented by combined SiO₂ and FeOT which shows an anti-correlation with CaO which represents the altered material. The John Klein values from the tailings, drill hole wall, and dump pile indicate a higher calcium sulfate composition; these measurements conflict with the values from the surface of the rocks, where the Cumberland site was much higher in calcium. This difference can be partly explained by the increased number of observations on the surface of Cumberland compared to the surface of John Klein, as more observations increase the likelihood of detecting the veins but this alone probably cannot explain the difference in observed vein abundance between the two sites. This is supported by the standard deviation of CaO for John Klein surface observations being 2.79 while the standard deviation of the Cumberland rock surface is 5.81; the greater variation in values indicate that the surface of Cumberland was less homogeneous than John Klein. The most likely explanation is that Cumberland contains a greater number of calcium sulfate veins. Table 3 is an attempt to provide greater insight into the concentration of calcium sulfate veins down the hole; in particular, the table demonstrates that the

calcium sulfate veins contribute more of the total CaO value at John Klein, ~28.8%, than at Cumberland, ~10%. ChemCam observed 5.0–5.8% CaO in the drill tailings from both sites; however, the dump pile values show John Klein with ~1.5% more CaO than Cumberland. The dump piles also differ in the calcium sulfate contribution to the total CaO value; the Cumberland dump pile has a small, ~0.5%, increase in contribution of CaO from calcium sulfates compared to the tailings while at John Klein the calcium sulfates contribute ~8% less to the total CaO of the dump pile. The dump pile values should be more in line with what was seen by CheMin as they come from the same region in the hole, but there is less data in the dump piles as there are only about 6 point locations in the John Klein dump pile and about 15 point locations in the Cumberland dump pile with only the first 10 shots at each location definitely being usable. There is some evidence of the Mg-rich component present beneath the surface in the drill hole, but these features are not as common as the calcium sulfates, despite both being fairly prominent at the surface. This suggests that either the Mg-rich ridges are less prominent in the subsurface or are more difficult to detect in the subsurface.

4.3. ChemCam's ability to characterize drill hole materials as a function of depth

ChemCam's ability to conduct multiple rapid spot analyses proved useful as the instrument was able to examine the tailings and the dump piles from both holes multiple times, and

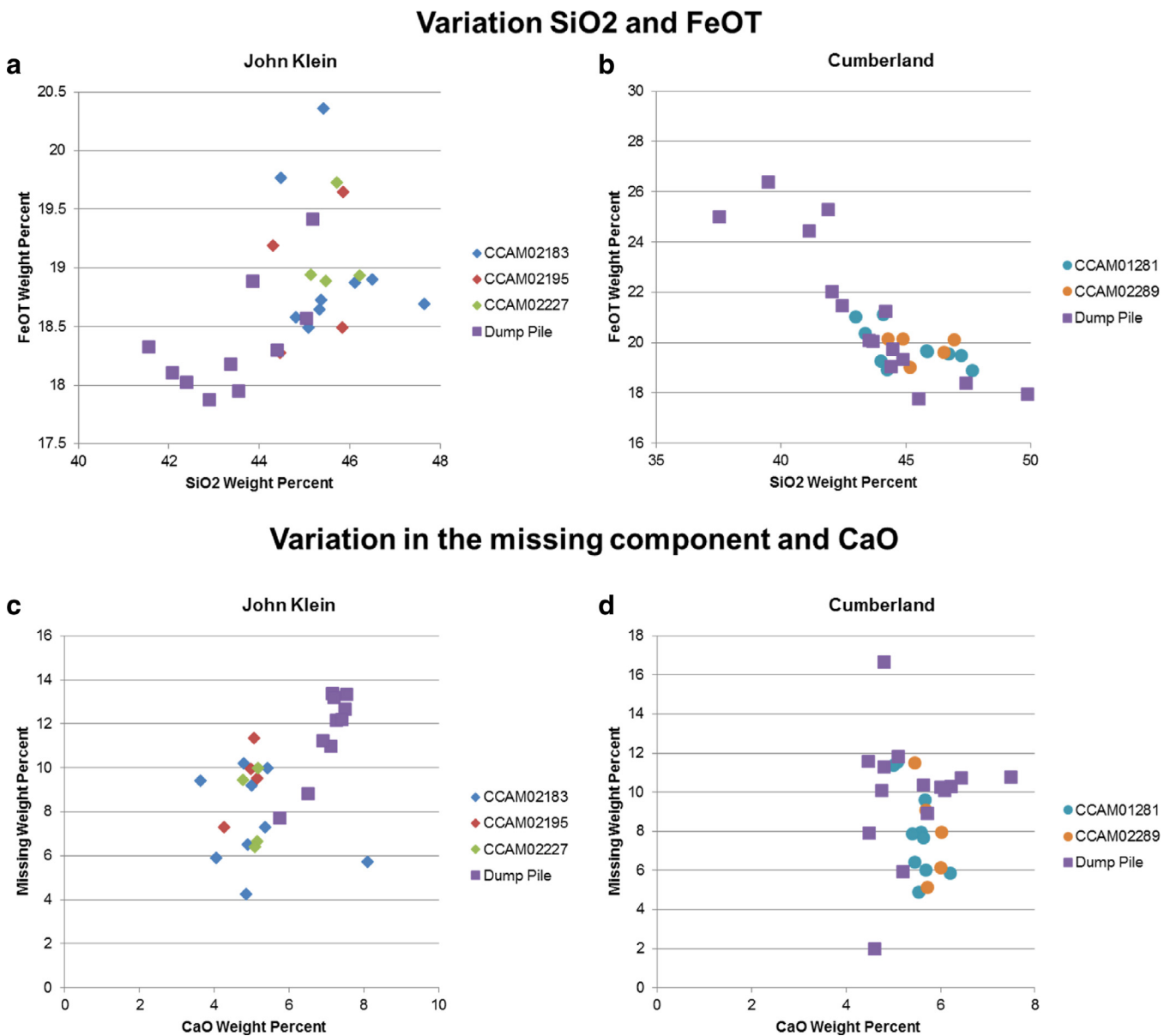


Fig. 10. (a) SiO₂ compared to FeOT displaying the John Klein drill tailings values with data from the dump pile, the averaged value of the first 10 shots are used to prevent incorporation of material under the dump pile. (c) SiO₂ compared to FeOT displaying the Cumberland values with the dump pile values included, the first 10 shots of the dump pile are used here. (d) CaO compared to Missing Component displaying John Klein drill tailing values, with the inclusion of the dump pile values, the first 10 shots of the dump pile are used here. (e) CaO compared to Missing Component displaying the Cumberland drill tailing values, with the inclusion of the dump pile values, the first 10 shots of the dump pile are used here.

comparison between the tailings and the dump pile provide a means to compare compositions of the top third and the middle third of the drill hole. While these two depth intervals are not very different in either drill hole, this could prove to be a useful analytical method in the future. As such, comparison of the tailings and the dump piles should most likely be done at every drill hole to compare these two intervals.

The multiple point analyses also allowed for detection and quantification of the diagenetic features, such as calcium sulfate veins and nodules, and the bulk unaltered mafic material, while other methods available to the rover measure a mixture of these groups. This allows ChemCam to provide a spatial context for the instruments that measure the bulk composition of the sample, such as SAM and CheMin; as well as, to identify and differentiate the geochemical components of the bulk material, Mg-rich ridges, and the calcium sulfates which comprise the bulk sample.

5. Conclusion

The drill tailings represent a mixture of basaltic sediments and diagenetic material predominantly consisting of calcium sulfates. The sediments and diagenetic materials are clearly distinguishable in both imaging and in compositions obtained from the drill hole walls, but the materials were mixed together during the drilling and sieving processes and were not distinguishable in the tailings or dump piles. There is no obvious surface alteration, as the red material on the top is air-fall dust; a red alteration layer in the top of the mudstone would have suggested that the depositional environment was oxidizing; however, the grey color of the mudstone suggests a more reducing environment during the original deposition of the sediments. The analyses suggest some differences with depth, especially at the John Klein site. As shown in Table 3 and Figs. 6, 7, and 9 there is a difference in the CaO

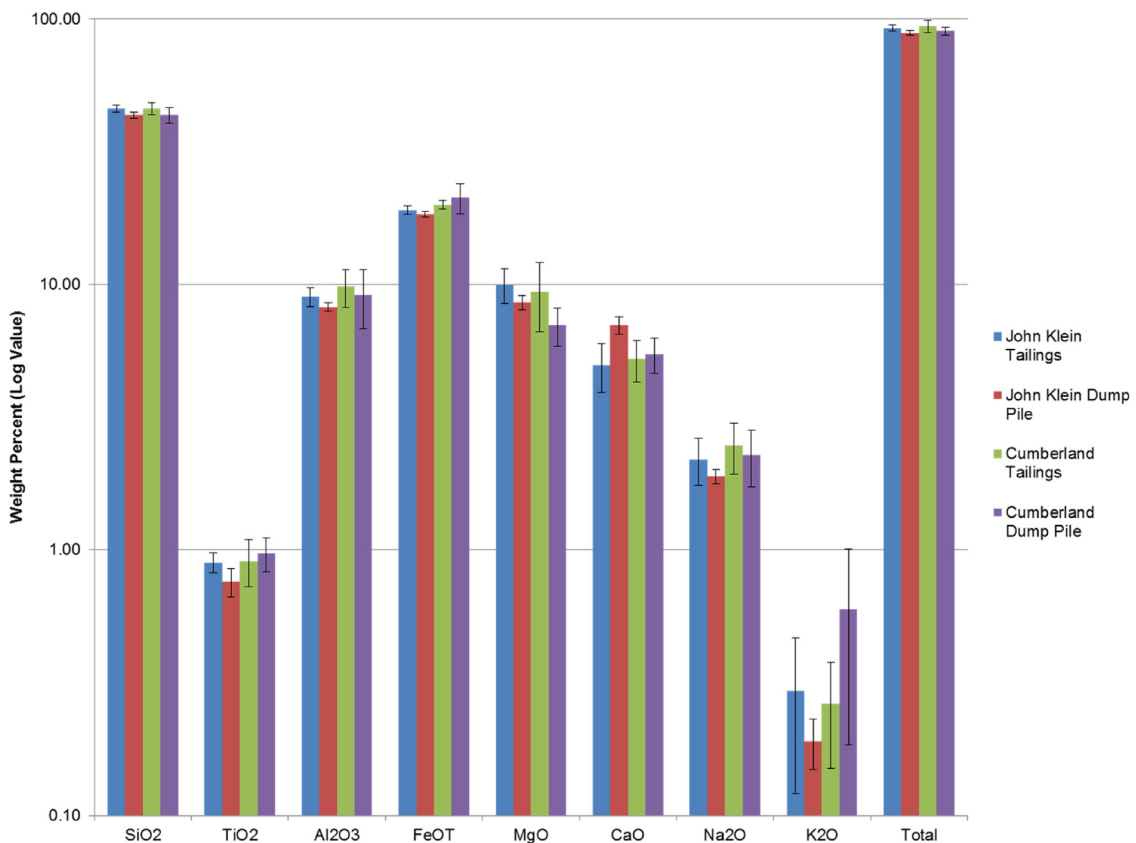


Fig. 11. The average values for the 8 oxides reported by the ChemCam data processing algorithm. Error bars are representative of 1 standard deviation, and dump pile values are the average of the first 10 shots, in order to avoid contamination from below.

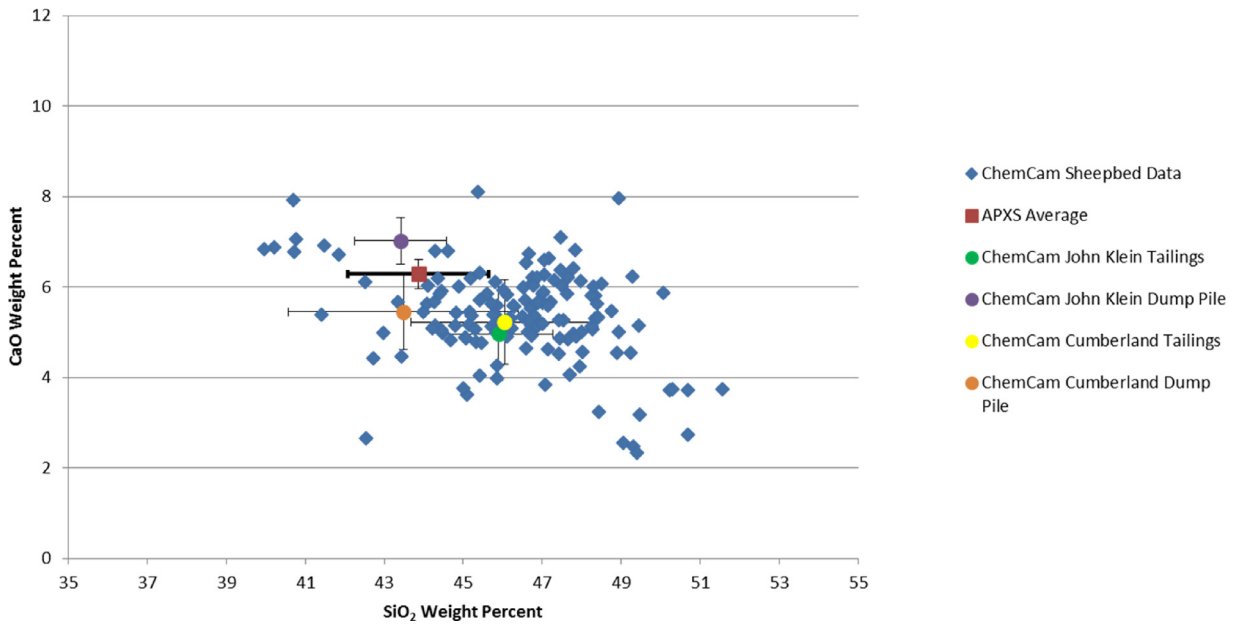


Fig. 12. Close up on the compositions of the Sheepbed mudstone, excluding the highest CaO features. There are several high CaO observations off to the top right that are not included in this graph, in order to focus on the bulk composition as reported by both APXS and ChemCam, but the high CaO observations are included in the ChemCam average data.

composition between material from the two drill holes and the surficial material. In John Klein the nominal abundances suggest less CaO, thus presumably less calcium sulfates, at the surface, with more CaO in the top 2 cm and even more from > 2 cm below the surface, but in Cumberland there is more CaO at the surface with less CaO down the drill hole which is consistent with the lack

of evidence of veins down the Cumberland drill hole. However, these differences between the drill sites and the top and middle thirds fall within 1 standard deviation of each other except for the difference between the John Klein tailings and the dump pile (Fig. 11). These differences indicate a greater amount of calcium sulfate material in the middle third of the John Klein Drill Hole, as

Table 3

Calculation of the percent of the total CaO reported by ChemCam that is needed to account for abundance of calcium sulfates quantified by CheMin from the internally analyzed samples. The total CaO from ChemCam is the average of all single shot data in the drill tailings. The data was rounded to the nearest three decimal places in order to avoid rounding mistakes.

Drill tailings			
John Klein			
CaO from ChemCam 5.07%	Weight ratio of CaO to total in Anhydrite 0.41	Weight ratio of CaO to total in Bassanite 0.36	Percent of the Ca in John Klein attributed to sulfates 28.31%
Cumberland			
CaO from ChemCam 5.78%	Weight ratio of CaO to total in anhydrite 0.41	Weight ratio of CaO to total in bassanite 0.36	Percent of the Ca in Cumberland attributed to sulfates 10.12%
Dump Pile			
John Klein			
CaO from ChemCam 7.02%	Weight ratio of CaO to total in Anhydrite 0.41	Weight ratio of CaO to total in Bassanite 0.36	Percent of the Ca in John Klein attributed to sulfates 20.44%
Cumberland			
CaO from ChemCam 5.45%	Weight ratio of CaO to total in Anhydrite 0.41	Weight ratio of CaO to total in Bassanite 0.36	Percent of the Ca in Cumberland attributed to sulfates 10.72%

is also suggested by the mapping from Fig. 8. However, as the drill sample is biased towards the middle third of the drill hole depth interval where the veins are more abundant, this indicates that the CheMin sample has a higher amount of calcium sulfate minerals than what is representative of the John Klein site. The similarity of composition between the top two thirds of Cumberland and the top third of John Klein is potentially due to the fact that the calcium attributed to calcium sulfates is a relatively minor fraction of the total calcium in the Sheepbed Mudstone (Table 3). At John Klein and Cumberland, we have demonstrated that the chemistry of the surface and the upper walls of the drill cores as analyzed by ChemCam are representative of the material introduced to CheMin and Sam. These analyses are also consistent with the chemistry of the material in the dump piles, which should be the best representation of the material examined by CheMin and SAM; however, there is much less material in the dump pile than the drill tailings. This lesser amount of dump pile material is not a great hindrance to analysis by ChemCam as the drill process seems to mix the material very well and ChemCam sampling of the dump pile should provide useable insights into the chemistry of the samples delivered to CheMin and SAM. Therefore, in the case of John Klein and Cumberland, where the only difference seen with depth is explainable by distribution of calcium sulfate veins, we have validated the approach of using the chemistry from the ChemCam and APXS to constrain the chemistry of individual mineralogical components determined by CheMin, such as the amorphous component (e.g. Morris et al., 2015).

Acknowledgments

This work was supported by the Mars Science Laboratory project, with additional support from the Centre National d'Etudes Spatiales (CNES) on the French part of the ChemCam project. In addition, the authors would like to thank JPL for designing and leading this successful mission. The lead author would also like to thank his wife and parents for their support.

References

- Anderson, R.C., Jandura, L., Okon, A.B., et al., 2012. Collecting samples in Gale Crater, Mars: an overview of the Mars Science Laboratory sample acquisition, sample processing and handling system. *Space Sci Rev* 170 (1–4), 57–75.
- Clegg, S.M., Sklute, E., Dyar, M.D., et al., 2009. Multivariate analysis of remote laser-induced breakdown spectroscopy spectra using partial least squares, principal component analysis, and related techniques. *Spectrochim. Acta Part B: Atomic Spectrosc.* 64 (1), 79–88.
- Clegg, S.M., Wiens, R.C., Anderson, R., et al., 2016. Recalibration of the Mars Science Laboratory ChemCam Instrument with an Expanded Geochemical Database. *Spectrochimica Acta Part B: Atomic Spectroscopy*, in preparation.
- Forni, O., Maurice, S., Gasnault, O., et al., 2013. Independent component analysis classification of laser induced breakdown spectroscopy spectra. *Spectrochim. Acta Part B: Atomic Spectrosc.* 86, 31–41.
- Gellert, R., Clark, B.C., 2015. In situ compositional measurements of rocks and soils with the alpha particle X-ray spectrometer on NASA's Mars Rovers. *Elements* 11 (1), 39–44.
- Gellert, R., Rieder, R., Brückner, J., et al., 2016. Alpha particle X-ray spectrometer (APXS): Results from Gusev crater and calibration report. *J. Geophys. Res.: Planets* 111 (E2).
- Grotzinger, J.P., Sumner, D.Y., Kah, L.C., et al., 2014. A habitable fluvio-lacustrine environment at Yellowknife Bay, Gale crater, Mars. *Science* 343 (6169), 1242777.
- Lanza, N.L., Ollila, A.M., Cousin, A., et al., 2015. Understanding the signature of rock coatings in laser-induced breakdown spectroscopy data. *Icarus* 249, 62–73.
- Le Mouélic, S., Gasnault, O., Herkenhoff, K.E., et al., 2015. The ChemCam remote micro-imager at Gale crater: Review of the first year of operations on Mars. *Icarus* 249, 93–107.
- Leveillé, R.J., Bridges, J., Wiens, R.C., et al., 2014. Chemistry of fracture-filling raised ridges in Yellowknife Bay, Gale Crater: Window into past aqueous activity and habitability on Mars. *J. Geophys. Res.: Planets* 119 (11), 2398–2415.
- Mangold, N., Forni, O., Dromart, G., et al., 2015. Chemical variations in Yellowknife Bay formation sedimentary rocks analyzed by ChemCam on board the Curiosity rover on Mars. *J. Geophys. Res.: Planets* 120 (3), 452–482.
- Maurice, S., Wiens, R.C., Saccoccia, M., et al., 2012. The ChemCam instrument suite on the Mars Science Laboratory (MSL) rover: science objectives and mast unit description. *Space Sci. Rev.* 170 (1–4), 95–166.
- McLennan, S.M., Anderson, R.B., Bell, J.F., et al., 2014. Elemental geochemistry of sedimentary rocks at Yellowknife Bay, Gale crater, Mars. *Science* 343 (6169), 1244734.
- Ming, D.W., Archer, P.D., Glavin, D.P., et al., 2014. Volatile and organic compositions of sedimentary rocks in Yellowknife Bay, Gale Crater, Mars. *Science* 343 (6169), 1245267.
- Morris, R.V., Ming, D.W., Gellert, R., et al., 2015. Update on the chemical composition of crystalline, smectite, and amorphous components for Rocknest soil and John Klein and Cumberland Mudstone Drill Fines at Gale Crater, Mars. In: *Lunar and Planetary Science Conference*, 46, p. 2622.
- Nachon, M., Clegg, S.M., Mangold, N., et al., 2014. Calcium sulfate veins characterized by ChemCam/Curiosity at Gale crater, Mars. *J. Geophys. Res.: Planets* 119 (9), 1991–2016.
- Okon, A., 2010. Mars science laboratory drill. In: *Proceedings of the 40th Aerospace Mechanisms Symposium*.
- Schröder, S., Meslin, P.Y., Gasnault, O., et al., 2015. Hydrogen detection with ChemCam at Gale crater. *Icarus* 249, 43–61. doi:10.1016/j.icarus.2014.08.029.
- Siebach, K.L., Grotzinger, J.P., Kah, L.C., et al., 2014. Subaqueous shrinkage cracks in the Sheepbed mudstone: Implications for early fluid diagenesis, Gale crater, Mars. *J. Geophys. Res.: Planets* 119 (7), 1597–1613.
- Stack, K.M., Grotzinger, J.P., Kah, L.C., et al., 2014. Diagenetic origin of nodules in the Sheepbed member, Yellowknife Bay formation, Gale crater, Mars. *J. Geophys. Res.: Planets* 119 (7), 1637–1664.
- Vaniman, D.T., Bish, D.L., Ming, D.W., et al., 2014. Mineralogy of a mudstone at Yellowknife Bay, Gale crater, Mars. *Science* 343 (6169), 1243480.
- Wiens, R.C., Maurice, S., Barraclough, B., et al., 2012. The ChemCam instrument suite on the Mars Science Laboratory (MSL) rover: Body unit and combined system tests. *Space Sci. Rev.* 170 (1–4), 167–227.
- Wiens, R.C., Maurice, S., Lasue, J., et al., 2013. Pre-flight calibration and initial data processing for the ChemCam laser-induced breakdown spectroscopy instrument on the Mars Science Laboratory rover. *Spectrochim. Acta Part B: Atomic Spectrosc.* 82, 1–27.